Aminoacid zwitterions in solution: Geometric, energetic, and vibrational analysis using density functional theory-continuum model calculations

Francisco R. Tortonda, Juan-Luis Pascual-Ahuir, Estanislao Silla,[a)]
and Iñaki Tuñón
Departamento de Química Física, Universidad de Valencia, 46100 Burjasot (Valencia), Spain

Francisco J. Ramírez
Departamento de Química Física, Universidad de Málaga, 29071 Málaga, Spain

Glycine and alanine aminoacids chemistry in solution is explored using a hybrid three parameters density functional (B3PW91) together with a continuum model. Geometries, energies, and vibrational spectra of glycine and alanine zwitterions are studied at the B3PW91/6-31+G** level and the results compared with those obtained at the HF and MP2/6-31+G** levels. Solvents effects are incorporated by means of an ellipsoidal cavity model with a multipolar expansion (up to sixth order) of the solute's electrostatic potential. Our results confirm the validity of the B3PW91 functional for studying aminoacid chemistry in solution. Taking into account the more favorable scaling behavior of density functional techniques with respect to correlated *ab initio* methods these studies could be extended to larger systems. © *1998 American Institute of Physics.*
[S0021-9606(98)30126-9]

I. INTRODUCTION

Nowadays, continuum models have become one of the more popular methods of incorporating solvent effects into theoretical calculations on chemical systems.[1] Although gas phase quantum calculations can frequently reproduce the essential features of chemical processes, there are a great variety of examples where the interaction with the surroundings must be explicitly included in order to obtain not only quantitative but also qualitative agreement with experiments.[2] Aminoacid chemistry in solution is clearly one of these examples. It is well known that glycine molecule, the smallest aminoacid, is found in its neutral form (NE) in the gas phase, whereas the zwitterionic form (ZW) dominates in crystalline or aqueous media.[3,4] *Ab initio* calculations using flexible basis sets show that the zwitterionic form is not an energy minimum *in vacuo*[5] and, consequently, if one wants to explore this aspect of the aminoacid chemistry, the interactions with the surroundings must be included into the calculations using, for example, continuum models. This is also the case of the analysis of the experimental infrared and Raman spectra of the aminoacids in solution.[6] The assignment of the different fundamental vibrations often needs accurate calculations on the zwitterionic form of the aminoacid, which can not be obtained without the consideration of the solvent-induced stabilization.

Previous theoretical works on aminoacids chemistry in solution have been usually restricted to the study of glycine zwitterion stability. Apart from statistical studies using classical potentials,[7] quantum mechanical studies have been carried out using either the continuum model[8–11] or small glycine-water clusters.[9,11,12] In a pioneer work using the continuum model, Tomasi *et al.*[8] showed that the electrostatic solute-solvent interactions stabilized the zwitterionic form, having this one an energy lower than the neutral form. Glycine zwitterion-water complexes have also been recently studied at ab initio levels. It seems that at least two water molecules are needed in order to transform the zwitterion into a local minimum.[9,12] However, the great number of degrees of freedom makes difficult the study of solute-solvent clusters with enough number of solvent molecules to correctly represent the solution. Continuum models offer a way to simplify the treatment of the solvent, the calculations being only slightly more expensive than *in vacuo*. In our previous study[9] on glycine zwitterion we showed that the long-range electrostatic interactions are needed to get a correct description of glycine energetics in solution and they are quite correctly incorporated into the continuum models. Continuum models have also been shown to be a useful tool for interpreting the vibrational spectra of aminoacid zwitterions in solution.[9,13] Nowadays, there is a great variety of continuum solvation models[1,14–17] and the selection of one of them must be based on the requirements of the system under study (semi-empirical or *ab initio*, punctual calculation or geometry optimizations, correlation energy, frequencies analysis ...).

From previous studies on the stability of the isolated glycine zwitterion,[5] it has been established that the correct description of the potential energy surface of the neutral-zwitterion aminoacid conversion demands a considerable computational effort. Small-size basis sets are not enough to determine whether the zwitterionic form is a minimum or not on the Hartree–Fock gas phase potential energy surface

---

[a)]Author to whom correspondence should be addressed. Electronic mail: Estanislao.Silla@uv.es

© 1998 American Institute of Physics

(PES). In this sense, the presence of polarization functions on hydrogen atoms is crucial.[5] Correlation energy seems also to play an important role. So, Ding *et al.*[11] concluded that there is not a zwitterionic minimum on the gas phase potential energy surface computed with a correlated wave function. In our recent study about glycine zwitterion[9] we showed that the complex of the zwitterion with a single water molecule is no longer a minimum when correlation energy is included at the second order of Møller–Plesset perturbation theory (MP2). However, when employing a continuum model the inclusion of correlation energy favors the zwitterionic form with respect to the neutral one, the former becoming the absolute minimum in solution, contrary to the results obtained at the Hartree–Fock level.

Thus moderate or large basis sets and correlation energy (for example, at the MP2 level) seem to be important factors to describe the zwitterion stability in solution. This kind of calculation can be nearly routinely made for glycine aminoacid but they can be very computationally demanding for larger aminoacids, especially if energy derivatives and force constants are required, and thus their application can be restricted to the smaller members of the series. Alternative methodologies are thus desirable. In this sense, density functional theory (DFT) methods explicitly include correlation energy and offer a way for obtaining accurate geometrical and thermodynamic data at a fraction of the computational cost of traditional correlated *ab initio* methods.[18] This is due to the favorable scaling behavior of DFT methods, opening up the way to studies on larger systems. Density functional methods have been previously applied to the study of the gas phase potential energy surface of glycine and alanine.[19,20] These studies show that standard density functional methods have some difficulties in reproducing the small energy differences among the different conformers found on the energy surface, but hybrid functionals, which include density gradient corrections and some Hartree–Fock exchange, approach the quality of MP2 calculations consuming less computational time. Promising results have also been obtained in the description of proton transfer processes when using such hybrid functionals.[21] It has also been recently shown that density functional methods in combination with the scaled quantum mechanical (SQM)[22] procedure successfully reproduce the vibrational spectra of a great variety of molecules, offering a useful tool for the interpretation and the assignment of the spectra of other systems.

In this paper we apply a density functional method in conjunction with a continuum solvation model to the study of the stability and vibrational dynamics of glycine and alanine zwitterions in solution. The results obtained with this method are compared with *ab initio* methods such as Hartree–Fock and MP2 calculations as well as with experimental results. We can state in advance that density functional methods give results of good quality and that together with the use of a continuum model can be very useful to predict and analyze the behavior of larger aminoacids in solution.

II. METHODOLOGY

Ab initio calculations have been carried out at the HF and MP2 levels using the $6\text{-}31+G^{**}$ basis set,[23] which includes polarization functions on all the atoms and diffuse functions on all the atoms but the hydrogens. Density functional theory calculations (DFT) have been made using the hybrid functional B3PW91.[24] This functional has been selected because it has been shown to behave better than the more usual hybrid B3LYP functional in the calculation of gas phase acidities.[25] Molecular geometries have been optimized at the respective levels using the Berny's and redundant coordinates algorithms.[26,27]

Solute-solvent electrostatic interaction has been simulated employing the continuum model of Rivail *et al.*[14,28,29] In this model, the liquid is assimilated to a continuum characterized by a dielectric constant (78.4 for water). The quantum system is then placed in an ellipsoidal cavity whose volume is obtained by means of an empirical relation.[30] The electrostatic interaction is calculated using a multipolar moment expansion (up to sixth order) and introduced in the Hamiltonian of the system. The analytical derivatives of this electrostatic term have been derived leading to an efficient geometry optimization procedure.[31] Cartesian force constants in solution have been calculated at the fully optimized geometry using analytical second derivatives.[32] This continuum model is probably the best choice if analytical force constants are required. It must be emphasized here that the more simplified Onsager's model[33] can lead to severe underestimations of the solute-solvent electrostatic interaction energy. For example, in the glycine zwitterion the dipolar term represents around 80% of the total interaction free energy, and 70% in the case of alanine. For larger aminoacids the participation of the dipolar term can be smaller (about 40% in the glutamine aminoacid).[34] All the calculations have been carried out using the GAUSSIAN94 package of programs.[35] For consideration of continuum solvent effects an extra link has been added.[36]

The cartesian force constants were transformed into a set of nonredundant local symmetrical internal coordinates, defined according to the Pulay methodology.[37] This allows for a more useful description of the vibrational potential energy, making comparisons for similar molecules easier. Wave numbers and normal coordinates were calculated by the Wilson FG matrix method.[38]

III. RESULTS

A. Geometries

The neutral and zwitterionic conformations of glycine and alanine studied in solution and the atom numbering are shown in Fig. 1 together with the transition structure connecting both structures. The neutral forms of the glycine and alanine present a large number of possible conformers[19,20,39] but the one shown in the Fig. 1 is the absolute minimum in solution both for glycine and alanine aminoacids.[9,40] These neutral structures are different from the absolute minima of the gas phase potential energy surface of glycine and alanine, but because of their large dipole moments, they become more stable than any other in solution. For the zwitterionic
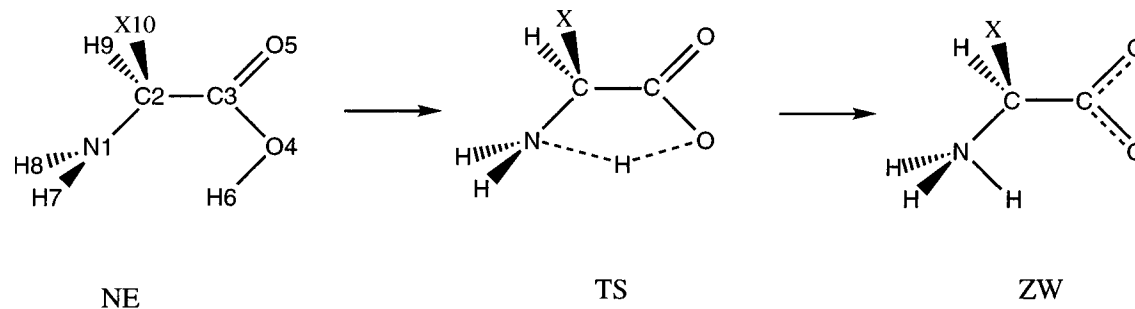
FIG. 1. Schematic representation and atomic numbering for the neutral, zwitterionic, and transition structure of the aminoacids here studied.

form of the two aminoacids we have not located any other minima structures in agreement with a previous study carried out in the gas phase.[5] The transition structure corresponds to the intramolecular proton transfer from neutral to zwitterionic aminoacid. From our previous results, it seems that the intramolecular proton transfer is energetically more favorable than the intermolecular proton transfer where a water solvent molecule directly participates in the transition structure.[9]

Selected geometrical parameters of the three structures studied in solution (NE, TS, and ZW) for glycine (X=H) and alanine (X=CH$_3$) are given in Table I. The geometrical parameters obtained for neutral glycine at the MP2 and B3PW91 levels are very close. As expected from the lack of correlation energy carbon−oxygen distances obtained at the HF level are too short. Another geometrical difference, with important consequences in the proton transfer process is the N1-H6 distance, much larger at the HF level (2.031 Å) than at the MP2 (1.821 Å) or B3PW91 (1.762 Å) levels. This seems to be a consequence of the loss of planarity among the H1−N−C−O2 atoms at the HF level. It has been previ-

TABLE I. Bond lengths (in Å), bond angles, and dihedral angles (in degrees) for the structures of glycine (X=H) and alanine (X=Me) studied at the different computational levels used.

			X=H						
	NE			TS			ZW		
	HF	MP2	B3PW91	HF	MP2	B3PW91	HF	MP2	B3PW91
C2N1	1.449	1.461	1.461	1.471	1.473	1.476	1.493	1.495	1.496
C2C3	1.521	1.526	1.529	1.534	1.537	1.541	1.540	1.546	1.551
C3O5	1.196	1.226	1.217	1.208	1.235	1.227	1.229	1.258	1.245
C3O4	1.315	1.341	1.331	1.277	1.313	1.300	1.241	1.274	1.267
C2X^{10}	1.084	1.089	1.094	1.080	1.087	1.092	1.082	1.087	1.090
O4H6	0.957	0.999	1.007	1.232	1.207	1.244	2.150	2.006	1.813
N1H6	2.024	1.821	1.762	1.255	1.313	1.275	1.010	1.031	1.048
N1C2C3	111.7	109.8	109.5	103.9	104.4	104.4	110.7	109.5	108.0
O5C2C3	122.7	123.8	124.0	121.5	122.3	121.7	115.0	115.3	115.6
O4C2C3	115.7	113.9	112.8	110.4	110.8	110.4	115.7	116.1	114.9
N1H6O4	120.0	128.9	128.9	140.8	141.3	141.1	109.7	117.5	124.8
N1C2C3O4	11.4	0.0	0.0	0.0	0.0	0.0	22.6	16.8	0.0
C2C3N1H6	9.1	0.0	0.0	0.0	0.0	0.0	29.5	18.0	0.0
			X=Me						
	NE			TS			ZW		
	HF	MP2	B3PW91	HF	MP2	B3PW91	HF	MP2	B3PW91
C2N1	1.453	1.465	1.467	1.478	1.479	1.484	1.505	1.504	1.510
C2C3	1.527	1.528	1.538	1.541	1.542	1.549	1.548	1.553	1.559
C3O5	1.197	1.226	1.218	1.209	1.235	1.228	1.233	1.264	1.251
C3O4	1.316	1.342	1.330	1.277	1.314	1.301	1.240	1.271	1.263
C2X10	1.535	1.531	1.532	1.529	1.527	1.528	1.532	1.527	1.530
O4H6	0.956	0.996	1.009	1.221	1.193	1.221	2.320	2.310	2.059
N1H6	2.068	1.857	1.750	1.292	1.327	1.292	1.008	1.023	1.031
N1C2C3	109.3	107.9	107.5	102.6	103.1	103.1	108.3	107.9	106.7
O5C2C3	123.0	124.0	124.0	121.7	122.5	121.9	115.7	116.0	116.2
O4C2C3	115.9	114.1	113.1	110.7	111.0	110.9	115.6	116.0	115.0
N1H6O4	117.7	126.2	130.4	140.7	141.0	141.1	103.0	105.4	114.7
N1C2C3O4	25.6	20.6	12.6	9.7	12.5	9.6	41.7	44.7	35.2
C2C3N1H6	19.7	16.3	10.0	6.9	9.4	7.0	44.6	42.9	29.7

ously established that the C_s structure (which has N1–C2–C3–O4 and H6–N1–C2–C3 dihedral angles equal to zero) is a transition state in the gas phase, connecting the two symmetrical C_1 structures[41,42] with an energy barrier of about 0.3 kcal/mol at the HF/6-311G** level[40] and only 0.1 kcal/mol when correlation energy is included at the MP2 level.[41,42] Solvent effects seem to diminish the force constant associated with the N1–C2–C3–O4 dihedral angle. So, the completely planar (C_s) structure has an energy only 0.03 kcal/mol higher than the nonplanar (C_1) one at the HF level and an imaginary frequency of 47 cm^{-1}. Conversely, geometry optimizations at the MP2 and B3PW91 levels (i.e., including correlation energy) which were started from different C_1 structures always led to the C_s one.

The transition structure of the intramolecular proton transfer is completely planar at the three computational levels used. This transition structure is more advanced in the reaction path at the HF and B3PW91 levels, with very similar N1–H6 and O4–H6 distances, than at the MP2 level where the NH1 distance is about 0.1 Å larger than the O4–H6 one. The N1–H6–O4 angle is about 140 degrees in the transition structure, approaching the linear hydrogen bond, while it was of about 120–130 degrees in the neutral form. This angle decreases again in the zwitterion, reaching a value between 109–125 degrees depending on the computational level. The more important difference among the geometries obtained for the glycine zwitterion at each computational level is the C_s symmetry structure obtained at the B3PW91 level, contrary to the HF and MP2 results. At the HF/6-31+G** level, the zwitterionic C_s structure is a transition state in solution with an imaginary frequency of 82 cm^{-1} and an energy 0.23 kcal/mol higher than the two mirror image C_1 structures. At the MP2 level, the differences are still smaller and the C_1 structures are only 0.04 kcal/mol more stable than the C_s one. We have optimized a C_1 zwitterionic structure at the B3PW91 level by keeping the N1–C2–C3–O4 dihedral angle fixed to the MP2 value. The resulting structure was 0.18 kcal/mol less stable than the C_s one. As a consequence of the planarity of the B3PW91 zwitterionic structure the intramolecular H6–O4 hydrogen bond is shorter at this computational level than at the HF and MP2 levels. In fact, the H6–O4 distance (1.813 Å) is shorter than at the HF (2.150 Å) and MP2 (2.006 Å) levels. We have also found the same results using the B3LYP hybrid functional. In the zwitterionic form, both carbon–oxygen bond lengths are very close, the C3–O4 bond length being somewhat larger because of the presence of the hydrogen bond with H6. In fact, the difference between both carbon–oxygen distances at each computational level is inversely proportional to the O4–H6 one. The carbon–carbon and the carbon–nitrogen bond lengths are larger in the zwitterion than in the neutral form of the glycine.

The geometrical description of the three structures (NE, TS, and ZW) for the alanine aminoacid is very similar to that for glycine. The main difference with respect to the glycine results arise from the presence of the methyl group breaking the possible symmetry of the structures. Effectively, in the case of alanine neither the neutral, the transition structure or the zwitterionic form present coplanarity among the H6–

TABLE II. Relative energies (in kcal/mol) for the structures of glycine (X=H) and alanine (X=Me) studied at the different computational levels used.

	X=H			X=Me		
	NE	TS	ZW	NE	TS	ZW
HF/6-31+G**	0.	11.04	2.29	0.	10.55	−0.45
MP2/6-31+G**	0.	2.39	−1.15	0.	2.16	−3.58
B3PW91/6-31+G**	0.	1.93	0.90	0.	1.32	−1.21

N1–C2–C3–O4 atoms at any of the computational levels here employed. Because of the hydrogen bond interaction, the transition structure is the closest to the planarity with N1–C2–C3–O4 dihedral angles ranging between 9 and 13 degrees, depending on the computational level. The intramolecular hydrogen bond O4–H6 is weaker in the zwitterionic form of the alanine than in the case of glycine. So, the O4–H6 distance is lengthened by 0.2–0.3 Å with respect to the glycine zwitterion, depending on the computational level. Consequently, the N1–H6 bond lengths are somewhat shorter in the alanine zwitterion than in the glycine zwitterion.

B. Energies

Relative energies for the neutral (NE), zwitterionic (ZW), and transition structure (TS) conformations of glycine and alanine aminoacids in solution are shown in Table II. In a first examination of our results we can observe that the presence of a methyl group in alanine makes the zwitterionic structure more stable than the neutral one at all the computational levels used. This is not the case of glycine where only at the MP2/6-31+G** level the zwitterion is the more stable tautomeric form in solution by 1.15 kcal/mol. The relative stabilisation produced by the methyl group in the alanine zwitterion with respect to the glycine zwitterion is 2.74, 2.43, and 2.11 kcal/mol at the HF, MP2, and B3PW91 levels, respectively. The energy barriers for the intramolecular proton transfer are somewhat smaller for alanine than for glycine at the three computational levels employed. Inclusion of correlation energy seems to be fundamental to correctly describe the proton transfer barrier. The energy barriers are approximately five times higher at the HF level than the corresponding values at the MP2 level. Calculations at the B3PW91 level are in general in good agreement with MP2 results both for proton transfer energy barriers and zwitterion relative energies. Our estimations of the stabilization energy for the tautomeric equilibrium between neutral and zwitterionic forms of glycine and alanine aminoacids at the HF, MP2 and B3PW91 levels are 2.29, −1.15, and 0.90 kcal/mol and −0.45, −3.38, and −1.21 kcal/mol, respectively. These relative free energies have not been obtained by direct experimental determination and estimations are only available for the case of the glycine aminoacid. An estimation for glycine based on the equilibrium constant for the ratio of the zwitterionic form to the neutral form in pure water at 298 K gives a relative free energy of −7.27 kcal/mol[43] with respect to the neutral form and an-

TABLE III. Symmetrized Pulay coordinates used in this work for the vibrational analysis of glycine.

Number[a]	Coordinate[b]	Symbol	Description
1	r_{12}	$n(CN)$	CN stretch
2	r_{23}	$n(CC)$	CC stretch.
3	r_{34}	$n(CO_2^-)$	CO_2^- stretch.
4	r_{35}	$n(CO_2^-)$	CO_2^- stretch.
5	$r_{29}+r_{210}$	$n_s(CH_2)$	CH_2 sym. stretch.
6	$r_{29}-r_{210}$	$n_a(CH_2)$	CH_2 antisym. stretch.
7	r_{16}	$n(NH)$	NH_3^+ stretch.
8	r_{17}	$n(NH)$	NH_3^+ stretch.
9	r_{18}	$n(NH)$	NH_3^+ stretch.
10	$2b_{435}-b_{234}-b_{235}$	$d(CO_2^-)$	CO_2^- bending
11	$b_{234}-b_{235}$	$w(CO_2^-)$	CO_2^- wagging
12	C_3 out-of-plane bending	$g(OCO)$	CO_2^- out-pl bending
13	$5b_{9210}-b_{123}$	$d(CH_2)$	CH_2 scissoring
14	$5b_{123}-b_{9210}$	$d(CCN)$	skeletal bending
15	$b_{329}-b_{3210}+b_{129}-b_{1210}$	$r(CH_2)$	CH_2 rocking
16	$b_{329}+b_{3210}-b_{129}-b_{1210}$	$w(CH_2)$	CH_2 wagging
17	$b_{329}-b_{3210}-b_{129}+b_{1210}$	$t(CH_2)$	CH_2 twisting
18	$b_{617}+b_{618}+b_{718}-b_{216}-b_{217}-b_{218}$	$d_s(NH_3^+)$	NH_3^+ antisym. bending
19	$2b_{718}-b_{617}-b_{618}$	$d_a(NH_3^+)$	NH_3^+ antisym. bending
20	$b_{617}-b_{618}$	$d_a(NH_3^+)$	NH_3^+ sym. bending
21	$2b_{216}-b_{217}-b_{218}$	$r(NH_3^+)$	NH_3^+ rocking
22	$b_{217}-b_{218}$	$r(NH_3^+)$	NH_3^+ rocking
23	N_1-C_2 torsion	$t(NH_3^+)$	NH_3^+ torsion
24	C_2-C_3 torsion	$t(CO_2^-)$	CO_2^- torsion

[a]Arbitrary numbering
[b]The atomic numbering is defined in Fig. 1. r_{ij} is the stretching vibration of the bond between atoms i and j. b_{ijk} is the in-plane bending vibration of the angle between atoms i, j, and k. f_i is the out-of-plane bending vibration of the atom i. t_{ij} is the torsion vibration with respect to the bond between atoms i and j, which were defined as described in Refs. 47, 48.

other estimation based on thermodynamic cycles and summation method gives a relative free energy of -7.67 kcal/mol.[44] The procedure employed in this last estimation implies the use of the summation method to obtain the solvation energy of some ions, which has been shown to produce large errors.[45]

The discrepancy between the experimental estimations and our theoretical values can be rationalized considering the different possible source of errors. First, our values are incomplete because of the lack of zero-point, thermal, dispersion-repulsion, and cavitation contributions to the relative free energy. It has been shown that the sum of thermal and dispersion-repulsion terms can favor the zwitterionic form of the glycine aminoacid by about 1.6 kcal/mol with respect to the neutral one in solution.[1] Although cavitation energies could be expected to be of similar magnitude for zwitterionic and neutral glycine, a diminution of the cavity is expected in the zwitterion because of the contraction of the solvent shell as a consequence of a stronger solute-solvent interaction. In fact, by means of QM/MM calculations[46] we have verified that the first peaks of the radial distribution functions (RDFs) of N1 and O4 atoms of the glycine zwitterion are shifted toward smaller distances by about 0.1 Å when compared with the neutral glycine RDFs. This contraction can also affect the rest of the solute-solvent interaction energy terms. Second, the cavity model (ellipsoidal) here used can also underestimate the electrostatic stabilization of the zwitterion. In fact, we have carried out a punctual calcu-

lation at the MP2 level using a molecular shaped cavity (by means of the PCM model[15]) and we have obtained a relative free energy of -4.85 kcal/mol, i.e., the zwitterion being 3.70 kcal/mol more stable than with the ellipsoidal cavity. This result could be further refined taking into account the change in the cavity volume due to the contraction of the solvation shell around the zwitterion with respect to the neutral form. As said above, the use of the ellipsoidal cavity model is here justified because we are also interested in obtaining analytic second derivatives.

C. Vibrational analysis

We have obtained complete quadratic force fields for glycine and alanine zwitterions at the absolute minimal energy structures each, using both HF and B3PW91 levels. The force constants were transformed to the set of locally symmetrized internal coordinates listed in Tables III and IV. The results concerning frequencies, infrared intensities, and potential energy distribution (P.E.D.) are summarized in Tables V and VI for glycine and alanine, respectively, where the experimental frequencies and assignments were included. Finally, diagonal force constants for the two aminoacids studied are compared in Table VII.

In spite of the fact that some glycine frequencies are not available from experiments, because of the strong water absorptions, the results listed in Table V show that the B3PW91 set of data are significantly improved with respect

TABLE IV. Symmetrized Pulay coordinates used in this work for the vibrational analysis of alanine.

Number[a]	Coordinate[b]	Symbol	Description
1	r_{12}	$n(CN)$	CN stretch
2	r_{23}	$n(CC)$	CC stretch..
3	r_{29}	$n(CC)$	CC stretch..
4	r_{34}	$n(CO_2^-)$	CO_2^- stretch.
5	r_{35}	$n(CO_2^-)$	CO_2^- stretch.
6	r_{210}	$n(CH)$	CH stretch.
7	r_{16}	$n(NH)$	NH_3^+ stretch
8	r_{17}	$n(NH)$	NH_3^+ stretch
9	r_{18}	$n(NH)$	NH_3^+ stretch
10	$r_{911}+r_{912}+r_{913}$	$n_s(CH_3)$	CH_3 sym. stretch.
11	$2r_{911}-r_{912}-r_{913}$	$n_a(CH_3)$	CH_3 antisym. stretch.
12	$r_{912}-r_{913}$	$n_a(CH_3)$	CH_3 antisym. stretch.
13	$2b_{435}-b_{234}-b_{235}$	$d(CO_2^-)$	CO_2^- bending
14	$b_{234}-b_{235}$	$w(CO_2^-)$	CO_2^- wagging
15	c_3 out of-plane bending	$g(OCO^-)$	CO_2^- out-pl bending
16	$2b_{3210}-b_{1210}-b_{9210}$	$d(CH)$	CH bending
17	$b_{1210}-b_{9210}$	d(CH)	CH bending
18	$4b_{321}-b_{329}-b_{921}$	$d(CCN)$	skeletal bending
19	$4b_{329}-b_{921}-b_{321}$	$d(CCN)$	skeletal bending
20	$4b_{921}-b_{321}-b_{329}$	$d(CCN)$	skeletal bending
21	$b_{617}+b_{618}+b_{718}-b_{216}-b_{217}-b_{218}$	$d_s(NH_3^+)$	NH_3^+ antisym. bending
22	$2b_{718}-b_{617}-b_{618}$	$d_a(NH_3^+)$	NH_3^+ antisym. bending
23	$b_{617}-b_{618}$	$d_a(NH_3^+)$	NH_3^+ sym. bending
24	$2b_{216}-b_{217}-b_{218}$	$r(NH_3^+)$	NH_3^+ rocking
25	$b_{217}-b_{218}$	$r(NH_3^+)$	NH_3^+ rocking
26	$b_{12913}+b_{12911}+b_{13911}-b_{2911}-b_{2912}-b_{2913}$	$d_3(CH_3)$	CH_3 antisym. bending
27	$2b_{12913}-b_{12911}-b_{13911}$	$d_a(CH_3)$	CH_3 antisym. bending
28	$b_{12911}-b_{13911}$	$d_a(CH_3)$	CH_3 sym. bending
29	$2b_{2911}-b_{2912}-b_{2913}$	$r(CH_3)$	CH_3 rocking
30	$b_{2912}-b_{2913}$	$r(CH_3)$	CH_3 rocking
31	N_1–C_2 torsion	$t(NH_3^+)$	NH_3^+ torsion
32	C_2–C_3 torsion	$t(CO_2^-)$	CO_2^- torsion
33	C_2–C_9 torsion	$t(CO_2^-)$	CH_3 torsion

[a]Arbitrary numbering.
[b]The atomic numbering is defined in Fig. 1. r_{ij} is the stretching vibration of the bond between atoms i and j. b_{ijk} is the in-plane bending vibration of the angle between atoms i, j, and k. f_i is the out-of-plane bending vibration of the atom i. t_{ij} is the torsion vibration with respect to the bond between atoms i and j, which were defined as described in Refs. 47, 48.

to the HF ones. First, vibrational frequencies are undoubtedly nearer to those experimental in the most of cases and, second, the description of the normal modes is clearer. These facts permit an easier comparison with the experimental frequencies and assignments and further refinement processes using a brief number of parameters.

As can be seen in Table V, the HF results overestimate the methylene vibrations by about 300 cm^{-1} (stretchings) and 150 cm^{-1} (bendings), while the DFT methodology reduces the deviations to about 150 cm^{-1} and less than 30 cm^{-1}, respectively. The three bending vibrations involving the CO_2^- group were predicted at 625, 578, and 498 cm^{-1} by the B3PW91 calculation, in a good agreement with the experimental frequencies, namely, 671, 585, and 507 cm^{-1}. The HF frequencies are 743, 636, and 517 cm^{-1}, having nonvanished contributions from the methylene rocking mode. In the same way, skeletal C2–C3 and C2–N1 stretching vibrations are also improved in the B3PW91 calculation. Concerning the carboxylate stretching modes, the symmetrical vibration is reported at 1412 cm^{-1}, whereas the antisymmetrical $n_a(CO_2^-)$ band is hidden behind the strong $d(H_2O)$

absorption. The predicted B3PW91 frequencies for these vibrations are 1381 and 1696 cm^{-1}, respectively. The last vibration has been measured at 1596 cm^{-1} in solid glycine,[49] and at similar frequencies for other aminoacids.[50] In solvated glycine we expect a frequency for this vibration not far from the frequency of the solid state and somewhat smaller than the calculated frequency of 1696 cm^{-1}. The source of this behavior is found in the interaction force constant between the two C–O stretching coordinates, which is systematically underestimated in quantum-mechanical calculations. This off-diagonal force constant has to be specifically corrected to adjust the theoretical carboxylate stretching frequencies to the experiments.

The ammonium vibrations have to be analyzed separately, because their experimental frequencies are not available. Only the symmetrical bending and one of the rocking vibrations have been observed, although the assignment of the former is not unambiguous.[51–54] On the other hand, the minimum energy structures obtained by the two methodologies present intramolecular interactions N1–H6···O4–C3, which are stronger for the B3PW91 geometry, as was dis-

TABLE V. 6-31+G**/SCRF frequencies (cm^{-1}), infrared intensities (km mol^{-1}), and normal mode descriptions, obtained for glycine zwitterion. Experimental frequencies have been included for comparison.

Experimental[a]		B3PW91			HF		
Freq.	Assig.	Freq.	IR int.	P.E.D. (greater than 10%)	Freq.	IR int.	P.E.D. (greater than 10%)
		3535	143.4	$100n_a(NH_2)$	3738	179.8	$100n(NH_3^+)$
		3454	171.8	$99n_s(NH_2)$	3686	255.8	$99n(NH_3^+)$
3016	$n_a(CH_2)$	3199	507.4	$100n_a(CH_2)$	3598	104.0	$99n(NH_3^+)$
2972	$n_s(CH_2)$	3135	0.3	$98n_s(CH_2)$	3354	5.2	$83n_a(CH_2),15n_s(CH_2)$
		3072	15.1	$95n(NH)$	3262	2.2	$85n_s(CH_2),17n_a(CH_2)$
		1696	373.9	$106n_a(CO_2^-)$	1794	215.8	$85d_a(NH_3^+)$
		1668	49.6	$97d_a(NH_3^+)$	1789	812.1	$77n_a(CO_2^-),32d_a(NH_3^+)$
1615	$d_a(NH_3^+)$	1636	56.0	$76d_a(NH_3^+),14d_s(NH_3^+)$	1770	394.7	$67d_a(NH_3^+),29n_a(CO_2^-)$
1444	$d(CH_2)$	1473	31.0	$91d(CH_2)$	1641	405.5	$94d_s(NH_3^+)$
		1440	478.5	$79d_s(NH_3^+),10n(CO_2^-)$	1604	1.6	$93d(CH_2)$
1412	$n_s(CO_2^-)$	1381	314.9	$62n_s(CO_2^-),24n(CC),15d(CO_2^-)$	1561	281.2	$41n_s(CO_2^-),25n(CO),24w(CH_2)$
1330	$w(CH_2)$	1330	27.7	$76w(CH_2)$	1476	169.0	$55w(CH_2),25n_s(CO_2^-)$
1320	$t(CH_2)$	1311	11.1	$62t(CH_2),18r(NH_3^+)$	1437	22.6	$58t(CH_2),14r(NH_3^+)$
1121	$r(NH_3^+)$	1104	133.7	$69r(NH_3^+),12w(CH_2)$	1202	4.3	$38r(NH_3^+),28t(CH_2),22r(CH_2)$
		1102	1.5	$49r(NH_3^+),16r(CH_2)$	1179	60.8	$61r(NH_3^+),31w(CH_2)$
1031	$n(CN)$	1002	16.6	$90n(CN)$	1064	10.8	$72n(CN)$
		934	28.2	$49r(CH_2),29r(NH_3^+),22g(OCO^-)$	989	41.1	$42r(NH_3^+),31r(CH_2),20g(OCO^-)$
897	$n(CC)$	869	111.6	$52n(CC),34d(CO_2^-)$	938	104.8	$34n(CC),32d(CO_2^-),13n(CN)$
671	$d(CO_2^-)$	675	9.9	$41d(CO_2^-),13W(CO_2^-),13n(CC)$	743	14.6	$28d(CO_2^-),20g(OCO^-),13r(CH_2)$
585	$W(CO_2^-)$	578	2.3	$76g(OCO^-)$	636	25.3	$44g(OCO^-),28r(CH_2),19d(CO_2^-)$
507	$g(CO_2^-)$	498	69.8	$40w(CO_2^-),18n(CC),16d(CO_2^-)$	517	40.9	$47w(CO_2^-)$
		316	0.0	$108t(NH_3^+)$	290	53.7	$65d(CCN)$
		271	118.5	$78d(CCN),52d(CO_2^-)$	203	6.5	$94t(NH_3^+)$
		53	0.6	$50t(NH_3^+),47t(CO_2^-)$	86	0.9	$67t(CO_2^-),35t(NH_3^+)$

[a]Experimental frequencies and assignments are taken from Ref. 51, except the frequency of 1615 cm^{-1} (Ref. 53).

cussed previously. This fact gives rise to a $n(NH)$ frequency, 3072 cm^{-1}, significantly lower than the rest, 3535 and 3454 cm^{-1}. Comparing these calculated values with the experimental ones for solid glycine, 3058 and 3152 cm^{-1}, we can expect a similar environment for the N–H bond involved in these vibrations. It is clear that the intermolecular hydrogen bond of solid glycine has been substituted by the intramolecular interaction previously mentioned. This result is not so enhanced in the HF results because the H···O distance is longer, 2.150 Å, than that of the B3PW91 structure, 1.813 Å. The question here is what happens in solution with a glycine molecule. The answer will not be apparent while the NH_3^+ vibrations have not been undoubtedly assigned; nevertheless, the two bending vibrations experimentally reported up to now, $d_a(NH_3^+)$ and $r(NH_3^+)$, indicate that interactions stronger than those directly produced by a continuum solvent would be present. They should also affect to the carboxylate moiety, but we would expect the spectral influences to be lower.

The qualitative features of the calculated infrared spectra can be seen in Fig. 2, displayed from data listed in the Table V. Apart from the drastic difference originated by the low-frequency $n(NH)$ vibration, the calculated B3PW91 intensities are lower than those obtained by HF methodology for the ammonium vibrations, higher for the carboxylate and skeletal vibrations and similar for the methylene vibrational modes. If we take into account only the normal mode descriptions these differences are not satisfactorily explained. Therefore they have to be found by comparing the atomic charges obtained in both methods. The Mulliken charge dis-

tribution of the HF calculation gives +0.324, +0.601, −0.806, and −0.731 to atoms C2, C3, O4, and O5, respectively, while the corresponding charges are +0.237, +0.367, −0.648, and −0.625 in the case of the B3PW91 calculation. The enhancement of the net charges in the heavy atoms (except N) is fully compatible with the calculated intensities. Experimental infrared intensities are not available because only Raman spectra of glycine solutions are reported.

The most of topics set out above for the vibrational dynamics of glycine can be applied to the alanine molecule, whose results are summarized in the Table VI. As can be observed, the agreement between the observed and the B3PW91 frequencies is satisfactory; in addition, the normal mode descriptions from the P.E.D., support the proposed assignments on the basis of experiments.[55] Taking into account that these assignments were based in selective deuterium exchanges in all the hydrogen atoms, the reached agreement confirms the availability of the hybrid functional B3PW91 in reproducing vibrational spectra of highly polar species in solution.

Compared with the B3PW91 results for glycine, a significant difference can be observed involving the ammonium moiety. As mentioned previously, an internal five-membered cycle stabilizes the structure of a glycine molecule, while in alanine the three hydrogen atoms from the ammonium group have more similar environments, as obtained from the B3PW91 structural optimization. This implies that the related stretching vibrations, $n(NH)$ will be strongly coupled, so that they will appear at different frequencies depending on their symmetries: a symmetrical and two antisymmetrical vi-

TABLE VI. 6-31+G**/SCRF frequencies[a] (cm^{-1}), infrared intensities (km mol^{-1}), and normal mode descriptions, obtained for alanine zwitterion. Experimental frequencies have been included for comparison.

Experimental[a]		B3PW91			HF		
Freq.	Assig.	Freq.	IR int.	P.E.D. (greater than 10%)	Freq.	IR int.	P.E.D. (greater than 10%)
		3545	99.7	$98n(NH_3^+)$	3756	187.4	$97n(NH_3^+)$
		3436	300.8	$100n(NH_3^+)$	3705	188.6	$101n(NH_3^+)$
		3333	185.2	$101n(NH_3^+)$	3614	126.2	$102n(NH_3^+)$
		3183	8.3	$92n(CH)$	3342	8.3	$97n(CH)$
3003	$n_a(CH_3)$	3154	2.1	$94n_a(CH_3)$	3280	6.3	$98n_a(CH_3)$
2993	$n_a(CH_3)$	3134	13.9	$97n_a(CH_3)$	3262	25.8	$97n_a(CH_3)$
2949	$n_s(CH_3)$	3059	18.4	$97n_s(CH_3)$	3195	23.2	$97n_s(CH_3)$
		1661	541.7	$56d_a(NH_3^+),49n(CO_2^-)$	1783	117.8	$94d_a(NH_3^+)$
1607	$n(CO_2^-)+d_a(NH_3^+)$	1653	586.5	$58d_a(NH_3^+),45n(CO_2^-)$	1768	47.2	$95d_a(NH_3^+)$
		1636	319.0	$71d_a(NH_3^+),24n(CO_2^-)$	1756	1624.3	$120n(CO_2^-)$
1480	$d_a(CH_3)$	1488	72.1	$77d_a(CH_3)$	1652	362.4	$99d_a(NH_3^+)$
1459	$d_a(CH_3)$	1482	46.4	$79d_a(CH_3)$	1613	86.2	$74d_a(CH_3)$
		1478	349.9	$73d_s(NH_3^+)$	1603	0.7	$92d_a(CH_3)$
1410	$n(CO_2^-)$	1415	123.1	$55d_s(CH_3),22n(CO_2^-)$	1564	199.6	$36n(CO_2^-),21d_a(CH_3),16n(CC)$
1375	$d_s(CH_3)$	1392	69.0	$46d_s(CH_3),28n(CO_2^-)$	1536	42.4	$83d_s(CH_3)$
1351	$d(CH)$	1378	104.4	$67d(CH),17n(CO_2^-)$	1511	73.4	$76d(CH)$
1301	$d(CH)$	1313	42.0	$61d(CH)$	1447	106.6	$60d(CH)$
1220	$r(NH_3^+)$	1194	11.5	$28r(NH_3^+),24r(CH_3),13d(CCN)$	1293	19.12	$8r(CH_3),25r(NH_3^+),17d(CCN)$
1145	$r(NH_3^+)$	1108	46.1	$35r(NH_3^+),27d(CH)$	1202	41.2	$22r(NH_3^+),21r(CH_3)$
1110	$n(CN)$	1087	13.5	$38r(CH_3),22n(CN),18n(CC)$	1177	15.0	$24r(CH_3),21n(CN),18n(CC)$
995	$r(CH_3)$	972	38.1	$37r(NH_3^+),31r(CH_3)$	1039	20.0	$36r(NH_3^+),33r(CH_3),14n(CN)$
1001	$n(CC)$	953	16.9	$56r(NH_3^+),22n(CC),19r(CH_3)$	1014	24.9	$52r(NH_3^+),26n(CC),15r(CH_3)$
922	$r(CH_3)$	885	45.8	$34n(CC),31n(CN),23r(CH_3)$	968	40.4	$35n(CC),22r(CH_3),19n(CN)$
850	$n(CC)$	820	47.9	$33d(CO_2^-),26n(CC),21n(CN)$	878	43.6	$34n(CN),24d(CO_2^-)$
775	$g(OCO^-)$	773	9.0	$70g(OCO^-)$	863	22.5	$62g(OCO^-)$
640	$d(CO_2^-)$	654	1.7	$34d(CCN),28d(CO_2^-),14w(CO_2)$	708	9.6	$31d(CCN),28d(CO_2^-),13w(CO_2)$
527	$w(CO_2^-)$	509	48.8	$29w(CO_2^-),21d(CCN),14d(CO_2^-)$	550	44.1	$28w(CO_2^-),19d(CCN),11d(CO_2^-)$
399	$d(CCN)$	349	12.6	$79d(CCN)$	368	11.5	$81d(CCN)$
283	$d(CCN)$	277	52.8	$89d(CCN),25w(CO_2^-)$	298	32.8	$75d(CCN),25w(CO_2^-)$
219	$d(CCN)$	260	26.1	$57d(CCN)$	274	34.8	$67d(CCN),17g(OCO^-)$
		235	1.4	$71t(CH_3),25t(NH_3^+)$	243	8.5	$81t(CH_3)$
		222	17.7	$64t(NH_3^+),22d(CCN),12t(CH_3)$	191	3.5	$102t(NH_3^+)$
		60	8.5	$76t(CO_2^-),24t(NH_3^+)$	80	4.2	$89t(CO_2^-),12t(NH_3^+)$

[a]Experimental frequencies and assignments are taken from Ref. 55.

brations. Because these bands can not be observed in solution, we have to obtain information from the $d(NH_3^+)$ bending modes. One of these has been reported at 1607 cm^{-1} as having a mixed character of $d_a(NH_3^+)$ and $n(CO_2^-)$.[56] To correlate it with the theoretical spectra we can choose among three frequencies in Table VI, namely, 1661, 1653, and 1636 cm^{-1}. At the light of the potential energy distribution, the aforementioned modes are involved in the three frequencies with nonnegligible contributions, in agreement with the previous assignment. For glycine molecule, the calculated B3PW91 values for the two $d_a(NH_3^+)$ vibrations were 1668 and 1636 cm^{-1}, close to those obtained for alanine. However, the symmetrical $d_s(NH_3^+)$ vibration is calculated with a difference of +48 cm^{-1}, as a consequence of the intramolecular interaction, that upshifts the stretching vibrations while the corresponding bending vibrations are downshifted.[57]

The experimental frequencies measured between 1500 and 1200 cm^{-1} for alanine solution have been calculated with differences ranging from 5 to 23 cm^{-1} when the DFT methodology was used. Normal mode descriptions are consistent with the reported assignments in all the cases. Results from the HF calculation overestimates the frequencies in this region by more than 100 cm^{-1}; although the normal mode descriptions can be well correlated with the B3PW91 results and the experimental assignments. Comparisons for frequencies smaller than 1000 cm^{-1} show the same trends as those previously discussed for glycine. We would like to emphasize that the agreement of DFT-observed frequencies for the three CO_2^- bending vibrations are as satisfactory as in glycine, thus supporting the validity of this methodology.

We have displayed the calculated infrared spectrum of solvated alanine in Fig. 3. There we can observe a very intense band in the HF spectrum that corresponds to a CO_2^- stretching vibration. Its intensity, 1621.3 km mol^{-1}, is twice that of the related vibration for glycine (see Table V), the calculated charge distribution being very similar for the two molecules. As regards the P.E.D. of the corresponding frequencies, we can see that for glycine the $n(CO_2^-)$ coordinates are distributed into two close frequencies, namely, 1787 and 1770 cm^{-1}, while for alanine the same coordinate describes a single frequency, 1756 cm^{-1}. The contribution of 120% indicates high off-diagonal negative terms in the P.E.D.

The calculated diagonal force constants are listed in the

TABLE VII. Diagonal force constants (in mdyn/Å) calculated for glycine and alanine.

Glycine				Alanine			
Coord.[a]	Symbol	HF	B3PW91	Coord.[a]	Symbol	HF	B3PW91
1	$n(CN)$	4.897	4.594	1	$n(CN)$	4.516	4.098
2	$n(CC)$	4.553	3.961	2	$n(CC)$	4.380	3.668
3	$n(CO_2^-)$	11.267	9.349	3	$n(CC)$	4.668	4.288
4	$n(CO_2^-)$	12.090	10.778	4	$n(CO_2^-)$	11.249	9.512
5	$n_s(CH_2)$	6.050	5.534	5	$n(CO_2^-)$	11.784	10.336
6	$n_a(CH_2)$	5.973	5.482	6	$n(CH)$	6.118	5.551
7	$n(NH)$	7.484	5.193	7	$n(NH)$	7.628	6.239
8	$n(NH)$	7.334	6.773	8	$n(NH)$	7.726	6.941
9	$n(NH)$	7.666	6.773	9	$n(NH)$	7.344	6.512
10	$d(CO_2^-)$	1.496	1.342	10	$n_s(CH_3)$	5.905	5.412
11	$w(CO_2^-)$	1.277	1.275	11	$n_a(CH_3)$	5.784	5.358
12	$g(OCO^-)$	0.597	0.491	12	$n_a(CH_3)$	5.744	5.298
13	$d(CH_2)$	0.932	0.815	13	$d(CO_2^-)$	1.476	1.273
14	$d(CCN)$	1.812	2.046	14	$w(CO_2^-)$	1.228	1.116
15	$r(CH_2)$	0.887	0.742	15	$g(OCO^-)$	0.614	0.502
16	$w(CH_2)$	0.829	0.710	16	$d(CH)$	0.784	0.664
17	$t(CH_2)$	0.792	0.705	17	$d(CH)$	0.890	0.767
18	$d_s(NH_3^+)$	0.678	0.607	18	$d(CCN)$	2.173	2.109
19	$d_a(NH_3^+)$	0.718	0.597	19	$d(CCN)$	1.751	1.523
20	$d_a(NH_3^+)$	0.719	0.662	20	$d(CCN)$	2.081	1.824
21	$r(NH_3^+)$	0.744	0.760	21	$d_s(NH_3^+)$	0.660	0.578
22	$r(NH_3^+)$	0.754	0.672	22	$d_a(NH_3^+)$	0.726	0.627
23	$t(NH_3^+)$	0.072	0.190	23	$d_a(NH_3^+)$	0.728	0.647
24	$t(CO_2^-)$	0.111	0.191	24	$r(NH_3^+)$	0.698	0.636
				25	$r(NH_3^+)$	0.684	0.606
				26	$d_s(CH_3)$	0.673	0.572
				27	$d_a(CH_3)$	0.667	0.579
				28	$d_a(CH_3)$	0.657	0.570
				29	$r(CH_3)$	0.751	0.642
				30	$r(CH_3)$	0.771	0.663
				31	$t(NH_3^+)$	0.064	0.100
				32	$t(CO_2^-)$	0.131	0.080
				33	$t(CH_3)$	0.115	0.003

[a]See Tables III and IV for coordinate descriptions.

Table VII. Off-diagonal terms are available from the authors on request. The general trend for both the DFT force constants are smaller than those calculated from HF methodology. There are few exceptions to this result; as a consequence of the N1–H6···O4–C3 interaction, the $t(NH_3^+)$ torsional force constant is higher in DFT than in HF calculation. For glycine, it goes from 0.072 (HF) to 0.190 (DFT)

mdyn/Å, while for alanine the values are 0.064 and 0.106 mdyn/Å, respectively. A significant increase is also obtained for the carboxylate torsional mode, which is more enhanced in glycine, while the $t(CH_3)$ torsional force constant of alanine follows the general trend. A higher decrease occurs for coordinate number 7 of glycine, $n(NH)$, which goes from 7.484 (HF) to 5.183 mdyn/Å (DFTAt), the light of the vibra-
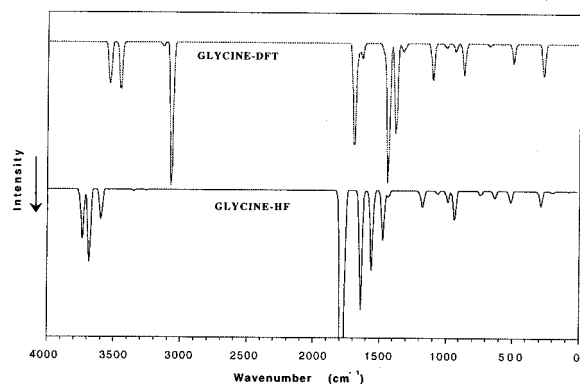

FIG. 2. HF/6-31+G** (HF) and B3PW91/6-31+G** (DFT) infrared spectra of glycine zwitterion in solution.
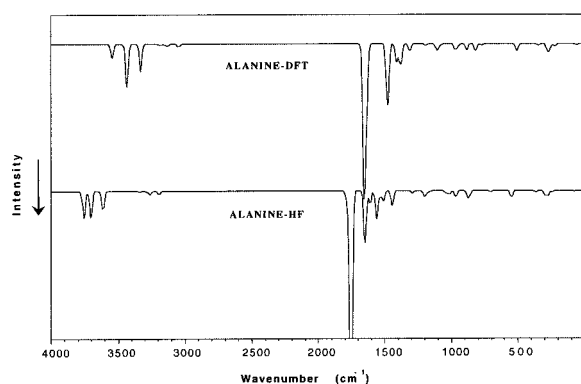

FIG. 3. HF/6-31+G** (HF) and B3PW91/6-31+G** (DFT) infrared spectra of alanine zwitterion in solution.

tional frequency comparison, previously discussed. We can postulate that a fitted value for a solvated ammonium N–H stretching force constant would be between the two values calculated for glycine by the DFT methodology, 5.193 and 6.703 mdyn/Å, which correspond to an hydrogen-bonded and a free N–H bond, respectively. The $n(CO_2^-)$ force constants also decrease appreciably for glycine and alanine on going from HF to DFT, while force constants for skeletal and nonpolar moieties are more similar.

IV. CONCLUSIONS

In this paper we have performed a thorough analysis of the performance of a hybrid-three parameters density functional (B3PW91) together with a continuum model to study different aspects of the aminoacid zwitterion chemistry in solution. Geometries, energies, and vibrational spectra of glycine and alanine aminoacid zwitterions have been studied at the B3PW91/6-31+G** level and the results compared with those obtained at the HF and MP2/6-31+G** levels. Solvents effects have been incorporated by means of an ellipsoidal cavity model with a multipolar expansion (up to sixth order) of the solute's electrostatic potential from which the analytical first and second derivatives can be readily obtained.

The geometrical parameters obtained at the B3PW91 and MP2 levels are very similar both for alanine and glycine. The main difference is found in the zwitterionic form of the glycine aminoacid. In this case MP2 calculations predict a C_1 structure while at the B3PW91 level a symmetric C_s structure is predicted as the absolute minimum. This discrepancy is due to very subtle energy differences. So, at the MP2 level the C_1 structure is only 0.04 kcal/mol more stable than the C_s one.

The energy values obtained at the B3PW91 level are also very close to the MP2 ones. HF calculations are shown to produce energy barriers for the neutral to zwitterion intramolecular conversion up to five times larger than when correlation energy is considered. A large part of the divergence with respect to experimental estimations of the glycine zwitterion stability seems to arise not from deficiencies of the density functional methodology but mainly to limitations of the selected cavity model. Results can be improved using a molecular-shaped cavity and fitting the atomic radii to the strength of the solute-solvent interactions. Further differences could be accounted for taking into account other unconsidered energy contributions.

The results from the vibrational analysis of glycine and alanine, and the comparison with the experimental spectra, demonstrate that the use of the B3PW91 density functional gives rise to a meaningful amelioration of the vibrational frequencies and normal mode descriptions of aminoacids in solution. We have also confirmed that specific intra- and/or inter-molecular interactions by hydrogen bonds play a non-vanished role in reproducing the vibrational behavior of these molecules.

We believe that the study here presented supports the validity of nonlocal density functionals, and in particular hybrid functionals, for obtaining good descriptions of aminoac-

ids chemistry in solution. Because of the lower computational cost of these calculations, density functional techniques are an interesting alternative to *ab initio* correlated methods for the theoretical study of bioorganic compounds such as aminoacids and polipeptids.

[1] (a) J. Tomasi and M. Persico, Chem. Rev. **94**, 2027 (1994); (b) C. J. Cramer and D. G. Truhlar, in *Reviews in Computational Chemistry*, edited by K. B. Lipkowitz and D. B. Boyd (VCH, New York, 1994); (c) J. L. Rivail and D. Dinaldi, in *Computational Chemistry. Reviews of Current Trends, Vol. 1*, edited by J. Leszczynski (World Scientific, Singapore, 1996).

[2] C. Reichardt, in *Solvents and Solvent Effects in Organic Chemistry* (VCH, New York, 1988).

[3] G. Albrecht and R. B. Corey, J. Am. Chem. Soc. **61**, 1087 (1939).

[4] P. G. Jonsson and A. Kvick, Acta Crystallogr., Sect. B: Struct. Crystallogr. Cryst. Chem. **28**, 1827 (1972).

[5] Y. Ding and K. Krogh-Jespersen, Chem. Phys. Lett. **199**, 261 (1992).

[6] M. W. Wong, K. B. Wiberg, and M. J. Frisch, J. Am. Chem. Soc. **114**, 523 (1992).

[7] (a) S. Romano and E. Clementi, Int. J. Quantum Chem. **14**, 839 (1978); (b) G. Alagona, C. Ghio, and P. A. Kollman, J. Mol. Struct.: THEOCHEM **166**, 385 (1988); (c) G. Alagona and C. Ghio, J. Mol. Model. **47**, 139 (1990).

[8] R. Bonaccorsi, P. Palla, and J. Tomasi, J. Am. Chem. Soc. **106**, 1945 (1984).

[9] F. R. Tortonda, J. L. Pascual-Ahuir, E. Silla, and I. Tuñón, Chem. Phys. Lett. **260**, 21 (1996).

[10] J. Andzelm, C. Kölmeland, and A. Klamt, J. Chem. Phys. **21**, 9312 (1995).

[11] Y. Ding and K. Krogh-Jespersen, J. Comput. Chem. **17**, 338 (1996).

[12] J. H. Jensen and M. S. Gordon, J. Am. Chem. Soc. **117**, 8159 (1995).

[13] (a) J. Casado, J. T. López-Navarrete, and F. J. Ramírez, J. Raman Spectrosc. **26**, 1003 (1995); (b) J. Casado, J. T. López-Navarrete, and F. J. Ramírez, Spectrochim. Acta A **51**, 2347 (1995).

[14] D. Rinaldi and J. L. Rivail, Theor. Chim. Acta **32**, 57 (1973).

[15] (a) S. Miertus, E. Scrocco, and J. Tomasi, Chem. Phys. **55**, 117 (1981); (b) R. Cammi and J. Tomasi, J. Comput. Chem. **16**, 1449 (1995); (c) E. L. Coitiño, J. Tomasiand, and R. Cammi, J. Comput. Chem. **16**, 20 (1995).

[16] C. J. Cramer and D. G. Truhlar, Science **256**, 213 (1992).

[17] A. Klamt and G. Schuurmann, J. Chem. Soc. Perkin Trans. **2**, 799 (1993).

[18] R. G. Parr and W. Yang, in *Density Functional Theory of Atoms and Molecules* (Oxford University Press, New York, 1989).

[19] (a) V. Barone, C. Adamo, and F. Lelj, J. Chem. Phys. **102**, 364 (1995); (b) D. T. Nguyen, A. C. Scheiner, J. W. Andzelm, S. Sirois, D. R. Salahub, and A. T. Hagler, J. Comput. Chem. **18**, 1609 (1997).

[20] A. G. Császár, J. Physiol. (London) **100**, 3541 (1996).

[21] V. Barone and C. Adamo, Int. J. Quantum Chem. **61**, 429 (1997).

[22] G. Rauhut and P. Pulay, J. Physiol. (London) **99**, 3093 (1995).

[23] (a) P. C. Hariharan and J. A. Pople, Theor. Chim. Acta **28**, 213 (1973); (b) T. Clark, J. Chandrasekhar, G. W. Spitznagel, and P. v. R. Schleyer, J. Comput. Chem. **4**, 294 (1983).

[24] (a) A. D. Becke, Phys. Rev. A **38**, 3098 (1988); (b) J. P. Perdew and Y. Wang, Phys. Rev. B **45**, 13244 (1992).

[25] G. N. Merrill and S. R. Kass, J. Physiol. (London) **100**, 17465 (1996).

[26] H. B. Schlegel, J. Comput. Chem. **3**, 214 (1982).

[27] C. Peng, P. Y. Ayala, H. B. Schlegel, and M. J. Frish, J. Comput. Chem. **17**, 49 (1996).

[28] J. L. Rivail and D. Rinaldi, Chem. Phys. **18**, 233 (1976).

[29] J. L. Rivail, D. Rinaldi, and M. F. Ruiz-López, in *Theoretical and Computational Models for Organic Chemistry*, edited by S. J. Formosinho, L. Arnaut and I. Csizmadia (Kluwer, Dodrecht, 1991).

[30] J. Bertrán, M. F. Ruiz-López, D. Rinaldi, and J. L. Rivail, Theor. Chim. Acta **84**, 181 (1992).

[31] D. Rinaldi, J. L. Rivail, and N. Rguini, J. Comput. Chem. **13**, 675 (1992).

[32] X. Assfeld and D. Rinaldi, in *AIP Conference Proceedings, ECCC 1*, edited by F. Bernardi and J. L. Rivail (AIP, Woodbury, NY, 1994).

[33] (a) L. Onsager, J. Am. Chem. Soc. **58**, 1486 (1936); (b) M. W. Wong, M. J. Frisch, and K. B. Wiberg, J. Am. Chem. Soc. **113**, 4776 (1991).

[34] F. J. Ramírez, E. Silla, and I. Tuñón (unpublished).

[35] M. J. Frisch, G. W. Trucks, H. B. Schlegel, P. M. W. Gill, B. G. Johnson, M. A. Robb, J. R. Cheeseman, T. Keith, G. A. Petersson, J. A. Montgomery, K. Raghavachari, M. A. Al-Laham, V. G. Zakrzewski, J. V. Ortiz, J. B. Foresman, J. Cioslowski, B. B. Stefanov, A. Nanayakkara, M. Challacombe, C. Y. Peng, P. Y. Ayala, W. Chen, M. W. Wong, J. L. Andres, E. S. Replogle, R. Gomperts, R. L. Martin, D. J. Fox, J. S. Binkley, D. J. Defrees, J. Baker, J. P. Stewart, M. Head-Gordon, C. Gonzalez, and J. A. Pople, GAUSSIAN 94, Revision D.3 (Gaussian, Inc., Pittsburgh, PA, 1995).

[36] D. Rinaldi and R. R. Pappalardo, SCRFPAC, QCPE Indiana University, Bloomington, IN, 1992. Program number 622.

[37] P. Pulay, G. Fogarasi, F. Pang, and J. R. Boggs, J. Am. Chem. Soc. **101**, 2550 (1979).

[38] E. B. Wilson, J. Chem. Phys. **7**, 1047 (1939).

[39] A. G. Császár, J. Mol. Struct. **346**, 141 (1995).

[40] As we show in Ref. 9 there is another conformer of neutral glycine that is 0.73 kcal/mol more stable in the gas phase at the MP2/6-31+G** than that presented in Fig. 1, but in solution the energy difference is −2.67 kcal/mol, at the same computational level, being the cyclic conformer of Fig. 1 more stable. In the case of alanine the energy difference in solution is −1.02 kcal/mol at the MP2/6-31+G** level. The energy barriers of the interconversion processes between both neutral conformers have been not considered.

[41] P. D. Godfrey and R. D. Brown, J. Am. Chem. Soc. **117**, 2019 (1995).

[42] R. F. Frey, J. Coffin, S. Q. Newton, M. Ramek, V. K. W. Cheng, F. A. Momany, and L. Schäfer, J. Am. Chem. Soc. **114**, 5369 (1992).

[43] G. Wada, E. Tamura, M. Okina, and M. Nakamura, Bull. Chem. Soc. Jpn. **55**, 3064 (1982).

[44] P. J. Haberfield, J. Chem. Educ. **57**, 346 (1980).

[45] M. J. Locke and R. T. McIver, Jr., J. Am. Chem. Soc. **105**, 4226 (1983).

[46] I. Tuñón, E. Silla, C. Millot, M. T. C. Martins Costa, and M. F. Ruiz-López (unpublished).

[47] J. A. Pople, R. Krishnan, H. B. Schlegel, D. J. DeFrees, J. S. Binkey, M. J. Frisch, R. F. Whiteside, R. F. Hout, and W. J. Hehre, Int. J. Radiat. Oncol., Biol., Phys. **15**, 269 (1981).

[48] G. Fogarasi and P. Pulay, Annu. Rev. Phys. Chem. **35**, 191 (1984).

[49] M. Kakihana, M. Akiyama, T. Nagumo, and M. Z. Okamoto, Z. Naturforsch. Teil A **43**, 774 (1988).

[50] M. Tsuboi, T. Takenishi, and A. Naramura, Spectrochim. Acta **18**, 271 (1963).

[51] K. Furik, V. Mohazed, M. Bonifazic, and I. Stefanic, J. Mol. Struct. **267**, 39 (1982).

[52] M. Takeda, R. E. S. Iavazzo, D. Garfinkel, I. H. Scheinberg, and J. T. Edsall, J. Am. Chem. Soc. **80**, 3813 (1958).

[53] S. A. S. Ghazanfar, D. V. Myers, and J. T. Edsall, J. Am. Chem. Soc. **86**, 3439 (1964).

[54] J. S. Alper, H. Dothe, and D. F. Coker, Chem. Phys. **153**, 51 (1991).

[55] M. Diem, P. L. Polavarapu, M. Oboodi, and L. A. Nafie, J. Am. Chem. Soc. **104**, 3329 (1982).

[56] J. F. Pearson and M. A. Slifrin, Spectrochim. Acta A **284**, 2403 (1972).

[57] L. J. Bellamy, in *Advances in Infrared Group Frequencies* (Methuen & Co., Ltd., Bungay, Suffolk, 1968).